Chemical Physics Letters 797 (2022) 139579

Contents lists available at ScienceDirect

Chemical Physics Letters

journal homepage: www.elsevier.com/locate/cplett

Implementation of solvent polarization in three-dimensional reference interaction-site model self-consistent field theory

Norio Yoshida [a,b,*], Tsuyoshi Yamaguchi [c], Haruyuki Nakano [a]

[a] Department of Chemistry, Graduate School of Science, Kyushu University, Motooka, Nishiku, Fukuoka 819-0395, Japan
[b] Graduate School of Informatics, Nagoya University, Chikusa, Nagoya 464-8601, Japan
[c] Graduate School of Engineering, Nagoya University, Chikusa, Nagoya 464-8603, Japan

ARTICLE INFO

Keywords:
Solvent-polarizable 3D-RISM
3D-RISM-SCF
Electronic structure theory
Solvent effects

ABSTRACT

The three-dimensional reference interaction-site model self-consistent field (3D-RISM-SCF) theory is an electronic structure theory of solvated molecules, which can handle the electronic polarization of the solute molecule induced by the interaction with the solvent, whereas the electronic polarization of solvent molecules is ignored. Here, the solvent-polarizable model is implemented to take into account the electronic polarization of solvent molecules. It is applied to the water molecule in an aqueous solution and the *p*-nitroaniline molecule in an aqueous solution, and the effects of the solvent polarization on the properties of these solutes are demonstrated.

1. Introduction

In chemical reactions in solution, the electronic structure change of the reactants induced by the solvent molecules is one of the key factors that govern the reactivity. At the same time, the solute electronic structure changes with the progress of the reaction, which in turn changes the polarization of the solvent molecules. For example, let us consider the electron-transfer reaction in solution according to Marcus's picture [1,2]. In the initial state, the solvent distribution and polarization are fully relaxed to minimize the free energy of the system. Solvent distribution and polarization change with the electron transfer of the solute reactants. The solvent distribution cannot respond immediately to a sudden change in the electronic structure of the solute, but the solvent polarization can. Then, with the progress of time, the solvent distribution relaxes and reaches the distribution with the minimum free energy for the product state. Therefore, a detailed description of the reaction process in solution requires a theory that can handle the electronic structure of the solute, solvent distribution, and solvent polarization.

The most straightforward way to describe the solute electronic structure and solvent polarization and distribution is to use an *ab initio* molecular dynamics method or quantum mechanics/molecular mechanics (QM/MM) method with polarizable solvent models [3]. These methods are, in general, very powerful, but it is difficult to sample sufficiently to calculate thermodynamic quantities due to their high computational cost. By contrast, the dielectric continuum model coupled with quantum chemical theories is a computationally efficient method [4–6]. This method treats the solvent as a continuous medium characterized by its dielectric constant. Using the static dielectric constant and the dielectric constant in the optical limit, the reorganization of the distribution and the electronic polarization of the solvent can be treated effectively.

Another candidate to handle the solvent effects on the solute electronic structure is the integral equation theory of molecular liquids, such as the reference interaction-site model (RISM), three-dimensional (3D) RISM, and molecular Ornstein–Zernike (MOZ) theories, and hybrid methods of these theories and electronic structure theory are called the RISM-self-consistent field (SCF), 3D-RISM-SCF, and MOZ-SCF theories, respectively [7–13]. The pioneering work to introduce solvent polarization into the RISM-SCF theory was performed by Naka and co-workers [14]. In their work, they employed the charge response kernel (CRK) to model the solvent polarization responding to the solute electronic structure change [15,16]. In their implementation, only the solute electrostatic potential affects the solvent polarization; therefore, the effect of the solvent polarized by the solute on the other solvents was ignored. To describe such an effect, it is necessary to evaluate the spatial solvent distribution around the solute, and it is desirable to adopt the

---

Abbreviations: RISM, reference interaction site model; SCF, self-consistent field; sp, solvent polarizable; DFT, density functional theory; CRK, charge response kernel.

[*] Corresponding author at: Department of Chemistry, Graduate School of Science, Kyushu University, Motooka, Nishiku, Fukuoka 819-0395, Japan.
E-mail address: noriwo@chem.kyushu-univ.jp (N. Yoshida).

https://doi.org/10.1016/j.cplett.2022.139579
Received 19 January 2022; Accepted 21 March 2022

3D-RISM theory, which can handle spatial distribution, instead of the RISM theory, which only handles the radial distribution.

Recently, the authors proposed the solvent-polarizable (sp-) 3D-RISM theory, which achieves the description of the solvent polarization induced by both solute and solvent based on the 3D-RISM theory coupled with the CRK method [17–19]. In this study, we propose a combined theory of the 3D-RISM-SCF and the sp-3D-RISM, which is referred to as the sp-3D-RISM-SCF theory. The method presented here enables us to take into account the electronic polarization of both solute and solvent molecules. The derivation of the formalism of sp-3D-RISM-SCF theory based on the free energy functional derivatives is presented first. The theory is then applied to the water molecule in aqueous solution and the *p*-nitroaniline (pNA) molecule in aqueous solution, and the effects of the solvent polarization on the properties of these solute molecules are demonstrated.

2. Theory

2.1. Free energy functional formalization

In the theory presented here, the electronic structure of a solute molecule immersed in a solvent at infinite dilution and its solvation structure as well as solvent charge polarization are evaluated. The solute electronic wavefunction, ψ, solvent distribution function, $g_v(\boldsymbol{r})$, and solvent polarization charge density, $\Delta Q_v(\boldsymbol{r})$, are determined to minimize the total free energy of the system, Ω_{tot}. The solvent polarization charge density is defined as $\Delta Q_v(\boldsymbol{r}) \equiv Q_v(\boldsymbol{r}) - Q_v^0$, where $Q_v(\boldsymbol{r})$ and Q_v^0 are the effective charge of solvent atom v at position $\boldsymbol{r}$ induced by the solute and that in the bulk solvent, respectively [20].

In this point of view, we propose a free energy functional formalization of the sp-3D-RISM-SCF theory. The total free energy of the system can be given by

$$\Omega_{\text{tot}}[\psi, \{g_v(\boldsymbol{r}), \Delta Q_v(\boldsymbol{r})\}] = \Omega_0[\{g_v(\boldsymbol{r})\}] + \Omega_{\text{pol}}[\{g_v(\boldsymbol{r}), \Delta Q_v(\boldsymbol{r})\}] + E_{\text{solu}}[\psi] + \sum_v \rho_v \int \left\{u_v^{\text{ne}}(\boldsymbol{r}) + V_{\text{solu}}[\psi;\boldsymbol{r}]\left(Q_v^0 + \Delta Q_v(\boldsymbol{r})\right)\right\} g_v(\boldsymbol{r}) d\boldsymbol{r}, \tag{1}$$

where Ω_0 denotes the free energy of the bulk solvent system without solvent polarization and Ω_{pol} is the additional contribution of solvent polarization. $E_{\text{solu}}[\psi] = \langle\psi|\widehat{H}_0|\psi\rangle$ is the solute electronic energy, where $\widehat{H}_0$ is an electronic Hamiltonian of the solute molecule in an isolated state. The fourth term corresponds to the solute–solvent interaction. $u_v^{\text{ne}}(\boldsymbol{r})$ gives a nonelectrostatic interaction, such as the Lennard-Jones (LJ) potential. $V_{\text{solu}}[\psi;\boldsymbol{r}] = \langle\psi|\widehat{V}_{\text{solu}}(\boldsymbol{r})|\psi\rangle$ is an electrostatic potential at position $\boldsymbol{r}$ induced by solute molecules, which functionally depends on the solute wavefunction, ψ. The requirement that $g_v(\boldsymbol{r})$, $\Delta Q_v(\boldsymbol{r})$, and ψ are determined to minimize Ω_{tot} leads to the following condition:

$$\delta\Omega_{\text{tot}} = \int\left\{\left[\frac{\delta\Omega_0}{\delta g_v} + \frac{\delta\Omega_{\text{pol}}}{\delta g_v} + \rho_v\left(u_v^{\text{ne}}(\boldsymbol{r}) + V_{\text{solu}}[\psi;\boldsymbol{r}]\left(Q_v^0 + \Delta Q_v(\boldsymbol{r})\right)\right)\right]\delta g_v + \left[\frac{\delta\Omega_{\text{pol}}}{\delta\Delta Q_v} + \rho_v V_{\text{solu}}[\psi;\boldsymbol{r}]g_v(\boldsymbol{r})\right]\delta\Delta Q_v\right\}d\boldsymbol{r} + \delta\left\langle\psi\left|\widehat{H}_0 + \sum_v \rho_v \int \widehat{V}_{\text{solu}}(\boldsymbol{r})\left(Q_v^0 + \Delta Q_v(\boldsymbol{r})\right)g_v(\boldsymbol{r})d\boldsymbol{r}\right|\psi\right\rangle = 0. \tag{2}$$

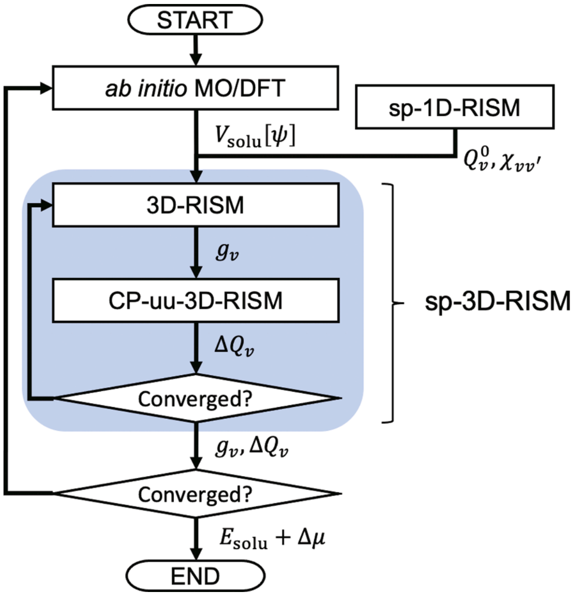

Scheme 1. Computational scheme of sp-3D-RISM-SCF theory. The blue background part corresponds to the sp-3D-RISM theory.

The first term in the integral for $\boldsymbol{r}$ on the right-hand side defines the solvent-polarizable 3D-RISM equation and the second term is for the polarization charge distribution. The last term on the right-hand side, the functional derivative with respect to ψ fixing g_v and ΔQ_v, defines the solvated Hamiltonian.

2.2. Solvent-polarizable 3D-RISM theory

From the first and second terms in eq. (2), the sp-3D-RISM equation and the polarization charge distribution $\Delta Q_v(\boldsymbol{r})$ are derived. $\Delta Q_v(\boldsymbol{r})$ is the polarization charge from the bulk solvent, which is given by

$$\rho_v g_v(\boldsymbol{r})\Delta Q_v(\boldsymbol{r}) = \sum_{v'} K_{vv'} \int \langle\rho_v(\boldsymbol{r})\rho_{v'}(\boldsymbol{r}')\rangle_{\text{s}} V(\boldsymbol{r}')d\boldsymbol{r}' = -\frac{\rho_v}{\beta}G_{vv}(\boldsymbol{r}), \tag{3}$$

where $\langle\rho_v(\boldsymbol{r})\rho_{v'}(\boldsymbol{r}')\rangle_{\text{s}}$ is the intramolecular density–density correlation function and $G_{vv}(\boldsymbol{r}) = \partial g_v(\boldsymbol{r})/\partial\gamma_v$ is the response of the distribution function for solvent charge perturbation parameter γ_v. $G_{vv}(\boldsymbol{r})$ is evaluated using the coupled-perturbed solute–solute (CP-uu-) 3D-RISM equation. The details of this formulation can be found in reference [17]. In the sp-3D-RISM theory, the electrostatic potential at position $\boldsymbol{r}$, namely $V(\boldsymbol{r})$, consists of the following three terms:

$$V(\boldsymbol{r}) = V_{\text{solu}}(\boldsymbol{r}) + V_{\text{solv}}^{\text{stat}}(\boldsymbol{r}) + V_{\text{solv}}^{\text{pol}}(\boldsymbol{r}). \tag{4}$$

$V_{\text{solv}}^{\text{stat}}(\boldsymbol{r})$ and $V_{\text{solv}}^{\text{pol}}(\boldsymbol{r})$ are given by

$$V_{\text{solv}}^{\text{stat}}(\boldsymbol{r}) = \sum_{v'} \int \rho_{v'} g_{v'}(\boldsymbol{r}') \frac{Q_{v'}^{0}}{|\boldsymbol{r}-\boldsymbol{r}'|} \text{erf}(\alpha|\boldsymbol{r}-\boldsymbol{r}'|) d\boldsymbol{r}', \tag{5}$$

$$V_{\text{solv}}^{\text{pol}}(\boldsymbol{r}) = \sum_{v'} \int \rho_{v'} g_{v'}(\boldsymbol{r}') \frac{\Delta Q_{v'}(\boldsymbol{r}')}{|\boldsymbol{r}-\boldsymbol{r}'|} \text{erf}(\alpha|\boldsymbol{r}-\boldsymbol{r}'|) d\boldsymbol{r}', \tag{6}$$

where α is a parameter introduced to exclude the self-interaction effectively [17].

The solute–solvent interaction potential to evaluate the solvent distribution function through the 3D-RISM equation is given by

$$u_v^{\text{CRK}}(\boldsymbol{r}) = u_v^{\text{LJ}}(\boldsymbol{r}) + Q_v^0 V_{\text{solu}}(\boldsymbol{r}) + \frac{1}{2}\delta\Delta Q_v(\boldsymbol{r})\left(V_{\text{solu}}(\boldsymbol{r}) + V_{\text{solv}}^{\text{stat}}(\boldsymbol{r}) + V_{\text{solv}}^{\text{pol}}(\boldsymbol{r})\right) + Q_v^0 V_{\text{solv}}^{\text{pol}}(\boldsymbol{r}). \tag{7}$$

This expression is derived from a comparison of the functional derivative of Ω_{tot} with respect to $g_v(\boldsymbol{r})$ with that of standard nonpolarized (np-) 3D-RISM [17]. Here, we employed the LJ potential u_v^{LJ} as a non-electrostatic potential u_v^{ne}. The spatial solvent distribution, $g_v(\boldsymbol{r})$, is obtained by solving the 3D-RISM equation with $u_v^{\text{CRK}}(\boldsymbol{r})$. Therefore, $g_v(\boldsymbol{r})$ and $\Delta Q_v(\boldsymbol{r})$ are determined by an iterative computational scheme.

The 3D-RISM equation should be solved coupled with a closure relation such as the hypernetted chain or the Kovalenko–Hirata closures [21]. The analytical expression for the solvation free energy, $\Delta\mu$, can be given as

$$\Delta\mu = \Delta\mu_{\text{sc}} + \Delta\mu_{\text{CRK}}, \tag{8}$$

$$\Delta\mu_{\text{CRK}} = -\sum_v \rho_v \int g_v(\boldsymbol{r}) \left(Q_v^0 + \frac{1}{2}\Delta Q_v(\boldsymbol{r})\right) V_{\text{solv}}^{\text{pol}}(\boldsymbol{r}) d\boldsymbol{r}, \tag{9}$$

where $\Delta\mu_{\text{sc}}$ is the Singer–Chandler formula for the solvation free energy [22].

The details of the CRK and sp-3D-RISM can be found in the previous papers [17,19].

2.3. sp-3D-RISM-SCF

A hybrid method of sp-3D-RISM and electronic structure theory, sp-3D-RISM-SCF, determines the solute electronic wave function, solvent distribution, and polarization charge density by solving the Schrödinger equation with the solvated Hamiltonian and the sp-3D-RISM iteratively, which is a similar manner to the former theories, such as Kohn–Sham density functional theory (KS-DFT)/3D-RISM or 3D-RISM-SCF [8,11,23,24].

The solute wave function, ψ, is determined using *ab initio* molecular orbital theory or KS-DFT by minimizing the expected value of the solvated Hamiltonian:

$$\varepsilon = \left\langle \psi \middle| \widehat{H}_0 + \sum_v \rho_v \int \widehat{V}_{\text{solu}}(\boldsymbol{r})\left(Q_v^0 + \Delta Q_v(\boldsymbol{r})\right) g_v(\boldsymbol{r}) d\boldsymbol{r} \middle| \psi \right\rangle, \tag{10}$$

$$\widehat{V}_{\text{solu}}(\boldsymbol{r}) = -\frac{e}{|\boldsymbol{r}-\boldsymbol{r}_e|} + \sum_u \frac{Z_u e}{|\boldsymbol{r}-\boldsymbol{r}_u|}, \tag{11}$$

where $\boldsymbol{r}_e$ and e are the coordinates of the electron and the elementary charge, respectively. Z_u and $\boldsymbol{r}_u$ are the nuclear charge and position of solute atom u, respectively. This condition is derived from the last term in eq. (2).

The computational scheme of sp-3D-RISM-SCF theory is shown in Scheme 1. Before the sp-3D-RISM-SCF iteration, an sp-1D-RISM calculation should be performed for the bulk solvent system to obtain the solvent susceptibility, $\chi_{vv'}$, and solvent effective charge, Q_v^0. At the beginning of the sp-3D-RISM-SCF iteration, we start from the electronic structure calculation of the solute molecule without solvent effects and obtain the electrostatic potential by the solute molecule, V_{solu}. Under the obtained V_{solu}, the sp-3D-RISM iteration consisting of 3D-RISM and CP-uu-3D-RISM is performed. The CP-uu-3D-RISM is introduced to obtain the response of the distribution function for the solvent charge perturbation, $G_{vv}(\boldsymbol{r})$, and hence one can obtain the polarization charge of the solvent, $\Delta Q_v(\boldsymbol{r})$, through eq. (3). The electrostatic potential acting on the solute electron due to the solvent molecules is evaluated using $g_v(\boldsymbol{r})$ and $\Delta Q_v(\boldsymbol{r})$, before proceeding to the next cycle. The iteration continues until the total free energy, $E_{\text{solute}} + \Delta\mu$, converges.

Table 1
Physical properties of H_2O in aqueous solution.

	DFT/ sp-3D-RISM	DFT/ np-3D-RISM	RHF/ sp-3D-RISM	RHF/ np-3D-RISM
E_{reorg} [kcal/mol]	2.55	2.26	2.73	2.41
$\Delta\mu$[kcal/mol]	–8.20	–7.61	–9.57	–8.92
$\Delta\mu_{\text{SC}}$ [kcal/mol]	–7.83	–7.61	–9.16	–8.92
$\Delta\mu_{\text{CRK}}$ [kcal/mol]	–0.37		–0.41	
Solute dipole moment [Debye]	2.64	2.61	2.77	2.74
Point charge on solute oxygen [e]	–0.952	–0.941	–0.998	–0.987

3. Computational details

In the present study, we examine two different systems, namely a solute H_2O molecule immersed in an aqueous solution and a pNA molecule in an aqueous solution. For both systems, the solute molecule is treated as a “quantum” molecule, whereas the solvent waters are treated as “classical” molecules.

The parameters for the solvent system are the same as in the previous study [17]. The water solvent is at 298.0 K with a number density of 0.0334 Å^{-3}. The LJ parameters for solvent water are taken from the simple point charge (SPC) model with a modified hydrogen parameter $\sigma_{\text{H}} = 1.00$ Å and $\varepsilon_{\text{H}} = 0.046$ kcal/mol [8,25]. The CRK and molecular structure of solvent water are taken from the literature [16]. The point charge of solvent water in vacuo is determined using the electrostatic potential method with the restricted Hartree–Fock/double zeta plus polarization (RHF/DZP) level.[26,27] The dielectric constant for the dielectric-consistent RISM calculation is set at 78.5 [28]. The number of grid points for computation of the neat solvent system is 2048 with a grid width of 0.05 Å.

For the solute molecules, the SPC LJ parameters are employed for the solute H_2O and the generalized Amber force field parameters for pNA [29,30]. The molecular structure of pNA is determined using the RHF/DZP method with an integral equation formula polarizable continuum model (PCM) calculation before the sp-3D-RISM-SCF calculation. For

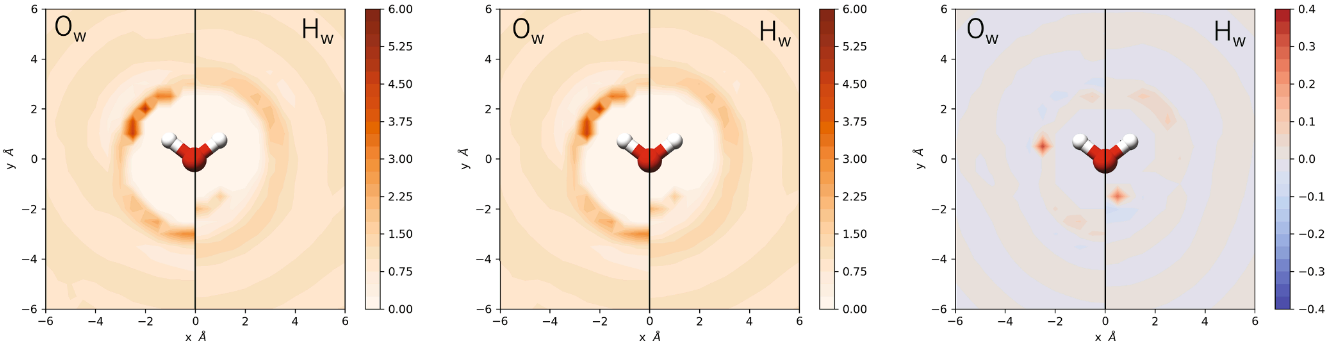

Fig. 1. Contour plot of solvent distribution functions around the solute water molecule. Left, center, and right panels are the distribution functions using sp-3D-RISM-SCF g_v^{sp}, np-3D-RISM-SCF g_v^{np}, and the difference between them, $g_v^{\mathrm{sp}} - g_v^{\mathrm{np}}$, respectively. The left and right parts in each panel correspond to distributions of oxygen and hydrogen, respectively.

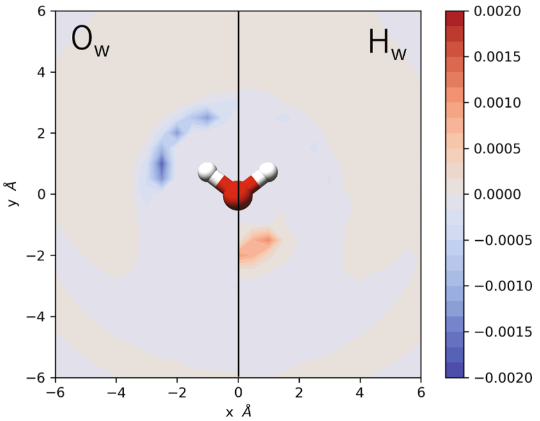

Fig. 2. Contour plot of polarized charge density of solvent water. The left and right parts correspond to distributions of oxygen and hydrogen, respectively.

Table 2
Physical properties of pNA in aqueous solution.

	DFT/ sp-3D-RISM	DFT/ np-3D-RISM	DFT/ PCM[a]	DFT/ gas phase
$\Delta\mu$[kcal/mol]	–3.30	–2.65	–6.13	
$\Delta\mu_{\mathrm{CRK}}$ [kcal/mol]	–0.64			
Solute dipole moment [Debye]	12.34	12.21	10.87	8.08
Solute dipole moment (FC state) [Debye]	14.97	13.94	17.16	12.47
π–π^* FC excitation energy [eV]	3.52	3.68	3.52	3.95
Solvation shift of π–π^* FC excitation energy [eV]	–0.43	–0.27	–0.43	

a) Evaluated using conductor-like PCM with iterative solver implemented in GAMESS.

the quantum chemical calculation of solute molecules, the DFT/DZP and RHF/DZP levels are employed for solute H_2O, and the DFT/DZP is used for solute pNA. For the Frank–Condon (FC) excited state, the time-dependent DFT with the DZP basis (TD-DFT/DZP) is employed. The functional of DFT and TD-DFT is the Becke, three-parameter, Lee–Yang–Parr (B3LYP) exchange–correlation functional.[31,32] In the FC state, the solvent distribution is fixed to that of the ground state, but the electronic polarization of the solvent is assumed to respond to the electronic excitation of the solute. The number of grid points for the 3D-RISM calculation is 128^3 with a grid width of 0.5 Å for both systems.

All the calculations were conducted using the RISM integrated calculator (RISMiCal) program package developed by us with the GAMESS quantum chemical program [33,34].

4. Results and discussion

A. H_2O in water

The sp-3D-RISM-SCF calculation for the H_2O molecule in water solvent was examined. In Table 1, the physical properties of the solute H_2O computed using sp-3D-RISM-SCF and conventional np-3D-RISM-SCF with KS-DFT and RHF are shown. The electronic polarization of solute H_2O is smaller in the DFT results than in the RHF. In both the DFT and RHF, with the introduction of the solvent-polarizable model, the polarization of the solute H_2O becomes larger. The solute electronic reorganization energy is defined as

$$E_{\mathrm{reorg}} = \langle \psi | \widehat{H}_0 | \psi \rangle - \langle \psi_0 | \widehat{H}_0 | \psi_0 \rangle, \tag{12}$$

where ψ_0 is the solute wave function in vacuo. The change in solute reorganization energy is 0.3 kcal/mol, whereas the solvation free energy change is –0.6 kcal/mol. Therefore, solvent polarization contributes to lowering the total free energy of the system, which is consistent with chemical intuition. According to eq. (8), the solvation free energy in sp-3D-RISM can be divided into the Singer–Chandler term, $\Delta\mu_{\mathrm{SC}}$, and the CRK term, $\Delta\mu_{\mathrm{CRK}}$. Both $\Delta\mu_{\mathrm{SC}}$ and $\Delta\mu_{\mathrm{CRK}}$ contribute to lowering the solvation free energy, and the $\Delta\mu_{\mathrm{CRK}}$ term shows a small but non-negligible contribution compared with $\Delta\mu_{\mathrm{SC}}$. The effects of solvent polarization on the solute electronic distribution can be seen in the solute dipole moment and the effective point charge on solute oxygen. Here, the effective point charges on the solute atoms were determined using the electrostatic potential method. The dipole moment was increased by about 0.03 Debye and the negative charge on the oxygen atom was increased by about 0.01 e.

In Fig. 1, contour plots of the distribution functions on the molecular plane evaluated using sp-3D-RISM-SCF g_v^{sp} and np-3D-RISM-SCF g_v^{np} are compared. Both sp- and np-3D-RISM-SCF show similar features of the distribution. The oxygen of solvent water shows a conspicuous peak around the solute hydrogen, whereas the solvent hydrogen shows a peak in the vicinity of solute oxygen. These features correspond to the hydrogen bond between water molecules. In the right panel of Fig. 1, the differences of the distribution functions by the sp- and np-3D-RISM-SCF, $g_v^{\mathrm{sp}} - g_v^{\mathrm{np}}$, are shown. The figure clearly shows that the introduction of solvent polarization enhances the hydrogen-bond feature. In addition, the distribution just outside the peak of hydrogen coordinated to the solute oxygen is lowered by the introduction of solvent polarization. This means that hydrogen bonding is enhanced by the induced polarization.

Fig. 2 shows the contour plot of polarization charge density, $\Delta Q_v(\boldsymbol{r}) g_v(\boldsymbol{r})$, on the molecular plane. The solvent oxygen making a hydrogen bond with solute hydrogen exhibits negative polarization induced by the positive charge on the hydrogen. By contrast, the hydrogen-bonded solvent hydrogen with the solute oxygen shows a positive charge distribution.

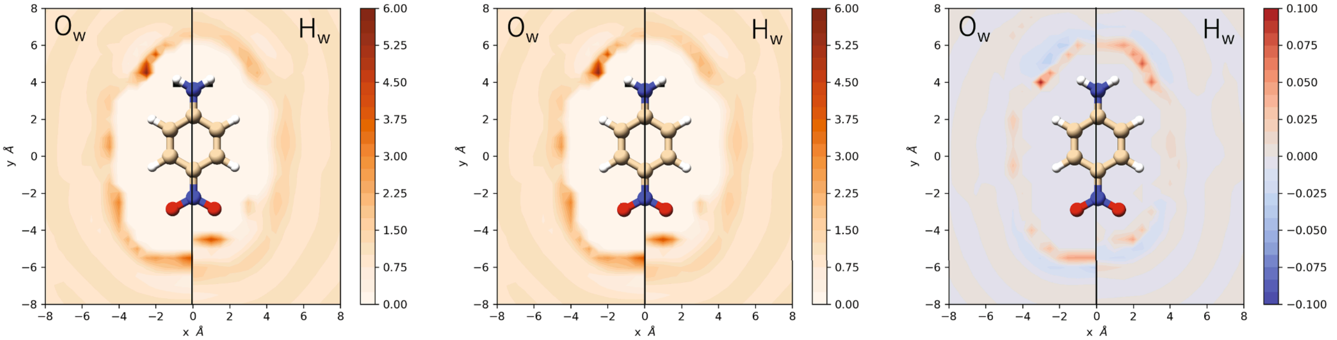

Fig. 3. Contour plots of solvent distribution functions around the solute pNA molecule. Left, center, and right panels are the distribution functions using sp-3D-RISM-SCF g_v^{sp}, np-3D-RISM-SCF g_v^{np}, and the difference between them, $g_v^{sp} - g_v^{np}$, respectively. The left and right parts in each panel correspond to distributions of oxygen and hydrogen, respectively.

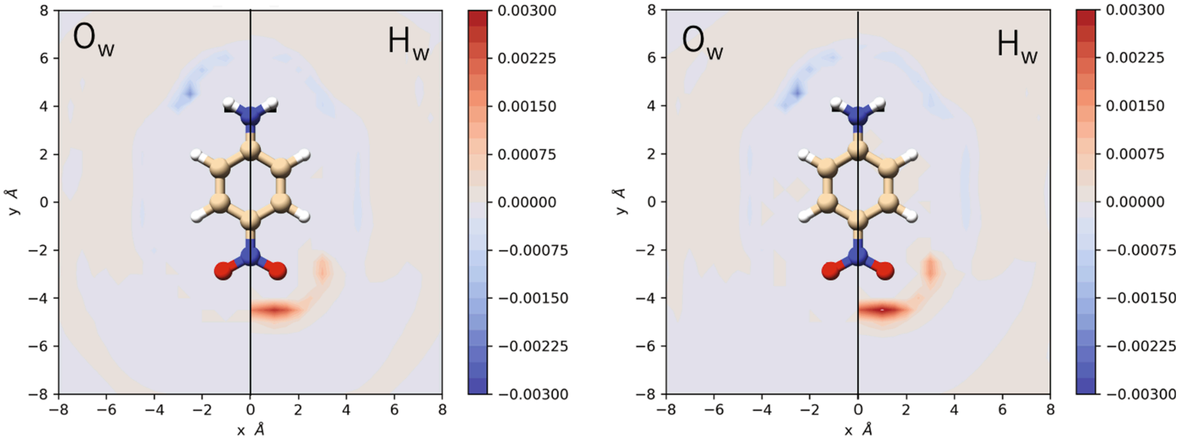

Fig. 4. Contour plots of the polarized charge density of solvent water. The left and right panels are those in the ground and FC states, respectively. The left and right parts correspond to distributions of oxygen and hydrogen, respectively.

B. *p*-Nitroaniline in water

The effect of the solvent polarization on the electronic structure of pNA in water was investigated by comparison with the np-3D-RISM-SCF and PCM. In Table 2, the physical properties of pNA in both the ground and excited states are summarized. As seen in the case of H_2O in water, the introduction of solvent polarization enhances the solute–solvent electrostatic interaction. The solvation free energy shows greater stabilization than the np-3D-RISM-SCF case. The dipole moments in the ground and π–π^* excited states are enhanced by the solvent effect, and especially the sp-3D-RISM-SCF shows the largest polarization in the solute. The change in the solute dipole moment is about 0.1 Debye in the ground state, whereas that in the π–π^* excited state is 1.0 Debye. In the π–π^* excited state, because pNA has charge separation, the effect of the polarization becomes larger. The π–π^* FC excitation energy is also examined. The FC excitation energy becomes smaller by the introduction of the solvent polarization. Because the electronic polarization of a solvent molecule can respond to the change of the solute electronic structure, the FC excitation energy with the solvent polarization becomes lower than that of a nonpolarizable model. According to this picture, the solvation shift of the π–π^* excitation energy of sp-3D-RISM-SCF shows a greater redshift than the np-3D-RISM-SCF. Compared with the experimental value, about –0.98 eV [35–37], np-3D-RISM-SCF underestimates the solvation shift, while the sp-3D-RISM-SCF improves it.

Fig. 3 compares the distribution functions on the molecular plane evaluated using sp-3D-RISM-SCF g_v^{sp} and np-3D-RISM-SCF g_v^{np} as contour plots. The conspicuous peak of the solvent oxygen can be found near the amino hydrogen. By contrast, a hydrogen peak appears around the nitro oxygen. Those peaks correspond to the hydrogen bond between solute pNA and solvent water. The change in g_v of pNA plotted in the left panel of Fig. 3 shows the effects of the introduction of solvent polarization on the solvent distribution. Similar to the H_2O system discussed in the previous subsection, the hydrogen-bond feature of the solvent distribution is enhanced by the solvent polarization, namely, the positive peak of oxygen around the amino hydrogen and that of hydrogen around the nitro oxygen. In Fig. 4, the polarization charge density distribution is plotted. The negative peak of oxygen and the positive peak of hydrogen are observed around the amino hydrogen and nitro oxygen, respectively. These features also indicate the enhancement of the solute–solvent electrostatic interaction by introducing solvent polarization. The polarization charge density distribution in the FC state is plotted in the right panel in Fig. 4. In this state, the solvent distribution, $g_v(\boldsymbol{r})$, is unchanged from the ground state, whereas the polarization charge, $\Delta Q_v(\boldsymbol{r})$, responds to the solute electronic structure change. The negative peak of oxygen around the amino hydrogen and the positive peak of hydrogen around the nitro oxygen seem to be greater than those in the ground state. As seen in Table 2, pNA in the π–π^* excited state has greater polarization, and hence both the positive and negative peak heights in the polarization charge density become greater than those in the ground state.

5. Summary

In this letter, we proposed a hybrid method of an electronic structure theory and the sp-3D-RISM theory to consider the electronic structure of solvated molecules as well as a solvation structure including solvent polarization.

The method was applied to the water molecule in aqueous solution and the pNA molecule in aqueous solution, and the effects of the solvent polarization on their properties were analyzed. The results clearly showed that solvent polarization has a nonnegligible effect on the electronic structure of the solute molecules. This indicates that taking solvent polarization into account allows for a more accurate description of chemical processes in solution, such as electron transfer.

Recently, we proposed a theory of nonequilibrium free energy using sp-3D-RISM and a theory of solvation dynamics [18,19]. By combining these theories with the sp-3D-RISM-SCF theory proposed in this study, we can obtain the solvation dynamics associated with the excitation energy transfer taking into account the polarization of solvent molecules. Such studies are in progress in the authors' group.

Declaration of Competing Interest

The authors declare the following financial interests/personal relationships which may be considered as potential competing interests: Norio Yoshida reports financial support was provided by Japan Society for the Promotion of Science. Haruyuki Nakano reports financial support was provided by Japan Society for the Promotion of Science. Tsuyoshi Yamaguchi reports financial support was provided by Japan Society for the Promotion of Science.

Acknowledgments

This work was supported by Grants-in-Aid from JSPS, Japan (Grant Nos. 18K05036, 19H02677, and 21K04980). Molecular graphics and analyses were performed with the UCSF Chimera package [38].

References

[1] R.A. Marcus, On the theory of oxidation-reduction reactions involving electron transfer. 1, J. Chem. Phys. 24 (5) (1956) 966–978.

[2] R.A. Marcus, Electrostatic free energy and other properties of states having nonequilibrium polarization. 1, J. Chem. Phys. 24 (5) (1956) 979–989.

[3] D. Frenkel, B. Smit, Understanding Molecular Simulation: From Algorithms to Applications, second ed., Academic Press, San Diego, CA, 2001.

[4] J. Tomasi, M. Persico, Molecular-interactions in solution - an overview of methods based on continuous distributions of the solvent, Chem. Rev. 94 (7) (1994) 2027–2094.

[5] C. Cramer, D.G. Truhlar, Implicit solvation models: equilibria, structure, spectra, and dynamics, Chem. Rev. 99 (8) (1999) 2161–2200.

[6] J. Tomasi, B. Mennucci, R. Cammi, Quantum mechanical continuum solvation models, Chem. Rev. 105 (8) (2005) 2999–3093.

[7] S. Ten-no, F. Hirata, S. Kato, A hybrid approach for the solvent effect on the electronic structure of a solute based on the RISM and Hartree-Fock equations, Chem. Phys. Lett. 214 (3–4) (1993) 391–396.

[8] S. Ten-No, F. Hirata, S. Kato, Reference interaction site model self-consistent-field study for solvation effect on carbonyl-compounds in aqueous-solution, J. Chem. Phys. 100 (10) (1994) 7443–7453.

[9] H. Sato, F. Hirata, S. Kato, Analytical energy gradient for the reference interaction site model multiconfigurational self-consistent-field method: application to 1,2-difluoroethylene in aqueous solution, J. Chem. Phys. 105 (4) (1996) 1546–1551.

[10] A. Kovalenko, F. Hirata, Self-consistent description of a metal–water interface by the Kohn-Sham density functional theory and the three-dimensional reference interaction site model, J. Chem. Phys. 110 (20) (1999) 10095–10112.

[11] H. Sato, A. Kovalenko, F. Hirata, Self-consistent field, ab initio molecular orbital and three-dimensional reference interaction site model study for solvation effect on carbon monoxide in aqueous solution, J. Chem. Phys. 112 (21) (2000) 9463–9468.

[12] N. Yoshida, S. Kato, Molecular Ornstein-Zernike approach to the solvent effects on solute electronic structures in solution, J. Chem. Phys. 113 (12) (2000) 4974–4984.

[13] N. Yoshida, H. Sato, Multiscale solvation theory for nano- and biomolecules, in: K. Nishiyama, T. Yamaguchi, T. Takamuku, N. Yoshida (Eds.), Molecular Basics of Liquids and Liquid-Based Materials, Springer Singapore, Singapore, 2021, pp. 17–37.

[14] K. Naka, A. Morita, S. Kato, Solvent electronic polarization effect on the electronic transitions in solution: charge polarizable reference interaction site model self-consistent field approach, J. Chem. Phys. 111 (2) (1999) 481–491.

[15] A. Morita, S. Kato, Ab initio molecular orbital theory on intramolecular charge polarization: effect of hydrogen abstraction on the charge sensitivity of aromatic and nonaromatic species, J. Am. Chem. Soc. 119 (17) (1997) 4021–4032.

[16] A. Morita, S. Kato, Molecular dynamics simulation with the charge response kernel: diffusion dynamics of pyrazine and pyrazinyl radical in methanol, J. Chem. Phys. 108 (16) (1998) 6809–6818.

[17] N. Yoshida, T. Yamaguchi, Development of a solvent-polarizable three-dimensional reference interaction-site model theory, J. Chem. Phys. 152 (11) (2020) 114108.

[18] T. Yamaguchi, N. Yoshida, Solvation dynamics in electronically polarizable solvents: theoretical treatment using solvent-polarizable three-dimensional reference interaction-site model theory combined with time-dependent density functional theory, J. Chem. Phys. 154 (4) (2021) 044504.

[19] T. Yamaguchi, N. Yoshida, Nonequilibrium free-energy profile of charge-transfer reaction in polarizable solvent studied using solvent-polarizable three-dimensional reference interaction-site model theory, J. Chem. Phys. 153 (3) (2020) 034502.

[20] In the previous papers, "$\delta\Delta Q_v$" was used to represent the polarization charge density, but for simplicity, we use "ΔQ_v" in the present paper.

[21] F. Hirata (Ed.), Molecular Theory of Solvation, Kluwer, Dordrecht, 2003.

[22] S.J. Singer, D. Chandler, Free energy functions in the extended RISM approximation, Mol. Phys. 55 (3) (1985) 621–625.

[23] S. Ten-No, F. Hirata, S. Kato, A hybrid approach for the solvent effect on the electronic-structure of a solute based on the RISM and Hartree-Fock equations, Chem. Phys. Lett. 214 (3–4) (1993) 391–396.

[24] A. Kovalenko, F. Hirata, Self-consistent description of a metal-water interface by the Kohn-Sham density functional theory and the three-dimensional reference interaction site model, J. Chem. Phys. 110 (20) (1999) 10095–10112.

[25] M.R. Reddy, M. Berkowitz, The dielectric constant of SPC/E water, Chem. Phys. Lett. 155 (2) (1989) 173–176.

[26] T.H. Dunning, Gaussian basis functions for use in molecular calculations. 1. Contraction of (9s5p) atomic basis sets for first-row atoms, J. Chem. Phys. 53 (7) (1970) 2823–2833.

[27] T.H. Dunning, P.J. Hay, Gaussian basis sets for molecular calculations, in: H. F. Schaefer (Ed.), Methods of Electronic Structure Theory, Springer US, Boston, MA, 1977, pp. 1–27.

[28] J. Perkyns, B.M. Pettitt, A dielectrically consistent interaction site theory for solvent—electrolyte mixtures, Chem. Phys. Lett. 190 (6) (1992) 626–630.

[29] J.M. Wang, R.M. Wolf, J.W. Caldwell, P.A. Kollman, D.A. Case, Development and testing of a general amber force field, J. Comput. Chem. 25 (9) (2004) 1157–1174.

[30] J. Wang, W. Wang, P.A. Kollman, D.A. Case, Automatic atom type and bond type perception in molecular mechanical calculations, J. Mol. Graph. Model 25 (2) (2006) 247–260.

[31] A.D. Becke, Density-functional thermochemistry. 3. The role of exact exchange, J. Chem. Phys. 98 (7) (1993) 5648–5652.

[32] C.T. Lee, W.T. Yang, R.G. Parr, Development of the Colle-Salvetti correlation-energy formula into a functional of the electron-density, Phys. Rev. B 37 (2) (1988) 785–789.

[33] N. Yoshida, The Reference Interaction Site Model Integrated Calculator (RISMiCal) program package for nano- and biomaterials design, IOP Conference Series: Materials Science and Engineering 773 (2020) 012062.

[34] M.W. Schmidt, K.K. Baldridge, J.A. Boatz, S.T. Elbert, M.S. Gordon, J.H. Jensen, S. Koseki, N. Matsunaga, K.A. Nguyen, S.J. Su, T.L. Windus, M. Dupuis, J. A. Montgomery, General atomic and molecular electronic-structure system, J. Comput. Chem. 14 (11) (1993) 1347–1363.

[35] S. Millefiori, G. Favini, A. Millefiori, D. Grasso, Electronic-spectra and structure of nitroanilines, Spectrochim. Acta A 33 (1) (1977) 21–27.

[36] C.L. Thomsen, J. Thogersen, S.R. Keiding, Ultrafast charge-transfer dynamics: studies of p-nitroaniline in water and dioxane, J. Phys. Chem. A 102 (7) (1998) 1062–1067.

[37] S. Sok, S.Y. Willow, F. Zahariev, M.S. Gordon, Solvent-induced shift of the lowest singlet pi -> pi* charge-transfer excited state of p-nitroaniline in water: an application of the TDDFT/EFP1 method, J. Phys. Chem. A 115 (35) (2011) 9801–9809.

[38] E.F. Pettersen, T.D. Goddard, C.C. Huang, G.S. Couch, D.M. Greenblatt, E.C. Meng, T.E. Ferrin, UCSF chimera - a visualization system for exploratory research and analysis, J. Comput. Chem. 25 (13) (2004) 1605–1612.